European Journal of
Nuclear
Medicine

Original article

Beta-particle dosimetry in radiation synovectomy

L.S. Johnson[1*], J.C. Yanch[1], S. Shortkroff[2], C.L. Barnes[2], A.I. Spitzer[2], C.B. Sledge[2]

[1] Department of Nuclear Engineering and Whitaker College of Health Sciences and Technology, Massachusetts Institute of Technology, 77 Massachusetts Avenue, Cambridge, MA 02139, USA

[2] Department of Orthopedic Surgery, Brigham and Women's Hospital, 75 Francis Street, Boston, MA 02115, USA

Received 1 November 1994 and in revised form 6 March 1995

Abstract. Beta-particle dosimetry of various radionuclides used in the treatment of rheumatoid arthritis was estimated using Monte Carlo radiation transport simulation coupled with experiments using reactor-produced radionuclides and radiachromic film dosimeters inserted into joint phantoms and the knees of cadavers. Results are presented as absorbed dose factors (cGy-cm^2/MBq-s) versus depth in a mathematical model of the rheumatoid joint which includes regions of bone, articular cartilage, joint capsule, and tissue (synovium) found in all synovial joints. The factors can be used to estimate absorbed dose and dose rate distributions in treated joints. In particular, guidance is provided for those interested in (a) a given radionuclide's therapeutic range, (b) the amount of radioactivity to administer on a case-by-case basis, (c) the expected therapeutic dose to synovium, and (d) the radiation dose imparted to other, nontarget components in the joint, including bone and articular cartilage.

Key words: Dosimetry – Radiation synovectomy – Monte Carlo simulation – Rheumatoid arthritis

Eur J Nucl Med (1995) 22:977–988

Introduction

Radiation synovectomy is a radiation therapy which has been used for more than 40 years to alleviate the pain and swelling of rheumatoid arthritis (RA) [1–3]. The procedure consists of the injection of a beta-emitting radionuclide into the joint capsule where it makes direct contact with the synovial membrane, or synovium. Phagocytic lining cells along the synovial surface quickly absorb some of the injected radioactivity from the capsule [4, 5]. Then, as the radionuclide decays, absorbed dose is imparted to the synovium. Provided the amount of radioactivity injected is sufficiently large to deliver a therapeutic dose to the tissue, it will be destroyed. Tissue which regenerates over time is expected to be asymptomatic for 2–5 years, and the progression of RA in the joint is thereby temporarily arrested. Benefits to patients include increased joint movement and reduced swelling, pain, and effusion. It is the purpose of this paper to report on the beta-particle dosimetry of eight radionuclides of interest in radiation synovectomy.

While the procedure has not been approved for general use in the United States (due to concern over excessive leakage of radioactivity from the joint), serious interest in radiation synovectomy persists (in Australia, Canada, the United States, and throughout Europe) [2]. For patients over 50 years of age with chronic, progressive RA, the treatment is especially attractive. Compared to surgical synovectomy, the radiation therapy is simpler and less troublesome for the patient; the period of admission is shorter; only local anesthesia is required; the cost is lower; and the duration of relief is comparable. After treatment, there are no problems with mobilization or flexion contractures of the joint. There is little danger of infection, and an operation can always be considered at a later date. Results of clinical trials, in general, are equally as appealing, with improvement reported in up to 100% of treated joints [6].

The "ideal" radionuclide has been considered to be a short-lived, low-energy beta-particle emitter with little or no coincident gamma-ray emission [7]. Low-energy beta particles are desirable because they typically deposit all of their kinetic energy within a few millimeters of tissue or less, a thickness which is on the order of the thickness of rheumatoid synovium. Short physical half-lives are desirable since leakage of radioactivity from the joint requires time, and nuclei which decay before leaking do not subject the patient to unnecessary extraarticular irradiation. Minimal gamma-ray emission can be used to monitor leakage of radioactivity away from the joint.

Before administration, the radionuclides typically are attached to larger molecules or particles to inhibit leak-

* *Present address:* Department of Radiation and Cellular Oncology, University of Chicago Medical Center, 5841 S. Maryland Avenue MC0085, Chicago, IL 60637, USA

Correspondence to: J.C. Yanch

age [2]. The resulting radiopharmaceutical must be small enough to be phagocytized by the surface layer of synovial lining cells, but not so small as to facilitate rapid biological removal from the joint. The most appropriate size range generally is considered to be 2–5 μm [8]. The radiopharmaceutical also should be biodegradable and easily removed from the joint after radioactive decay.

In the past, the radiopharmaceuticals most commonly injected have been inorganic colloids. Unfortunately, leakage of these colloids from the joint has sometimes led to significant radiation doses to the liver, spleen, and draining inguinal lymph nodes [9]. Recent advances in radiopharmaceutical design and synthesis, however, could eventually lead to a new class of radiation synovectomy agents which will exhibit minimal leakage of activity from the treated joint [10, 11]. Given these advances, and the lack of a cure for RA, some feel that the utility and practice of this important radiotherapy are likely to expand [2]. Accurate methods for estimating absorbed dose distributions in treated joints are therefore of interest.

In a previous paper [12], absorbed dose profiles were presented for six radionuclides of interest in radiation synovectomy: phosphorus-32, yttrium-90, dysprosium-165, holmium-166, rhenium-186, and gold-198. The profiles were generated using computer simulation of radiation transport in a mathematical model of the rheumatoid knee, the joint most commonly treated using radiation. Results of the simulations revealed the absorbed dose penetration of each of the six radionuclides in the model. Presented as absorbed dose per unit activity (Gy/mCi) versus distance (mm) in the model, the profiles can be used to extrapolate absorbed dose distributions in treated knees, or other *large* joints.

Since publication of the paper, the dosimetry of two additional radionuclides has been investigated using radiation transport simulation. Results are presented here. These two radionuclides, samarium-153 and rhenium-188, are attractive choices for use in radiation synovectomy due to their favorable chemistry, half-lives (46.8 h and 16.8 h, respectively), and beta-particle emission energies (average energies of 0.233 MeV and 0.776 MeV, respectively). In addition, absorbed dose profiles for the six radionuclides previously investigated have been revised and are presented in an improved format here. Use of the revised profiles allows one to extrapolate absorbed dose *and* dose rate distributions, not only in large joints but in small and medium joints as well. A more sophisticated approach to the effects of leakage of radioactivity away from the joint on the dosimetry is also included.

To verify the accuracy of the computer-generated beta-dose distributions, an experimental investigation of beta dosimetry in radiation synovectomy was completed as well. The experiments were conducted using radiachromic film dosimeters and two reactor-produced radionuclides, ^{165}Dy and ^{166}Ho, inserted into either joint phantoms or the knees of fresh, human cadavers. The joint phantoms were built to resemble the mathematical joint model as closely as is possible and used to measure depth-dose data in bone-, articular cartilage-, and tissue-equivalent materials. The cadavers were used to measure absorbed dose distributions in actual knees. For both sets of experiments, comparisons of measured data with the Monte Carlo predictions of beta-dose distributions in treated joints were made.

Materials and methods

Monte Carlo simulations

Mathematical joint model

The mathematical model used to calculate beta dosimetry in radiation synovectomy is a planar model of the rheumatoid joint. It is shown in Fig. 1 along with an inset which illustrates the highly irregular nature of convoluted synovium. Variabilities in the shape of convoluted synovium were considered to be too joint-specific to model explicitly.

In the model, bone (lined at the surface with 1 mm articular cartilage) is separated by the joint capsule (or joint cavity) from

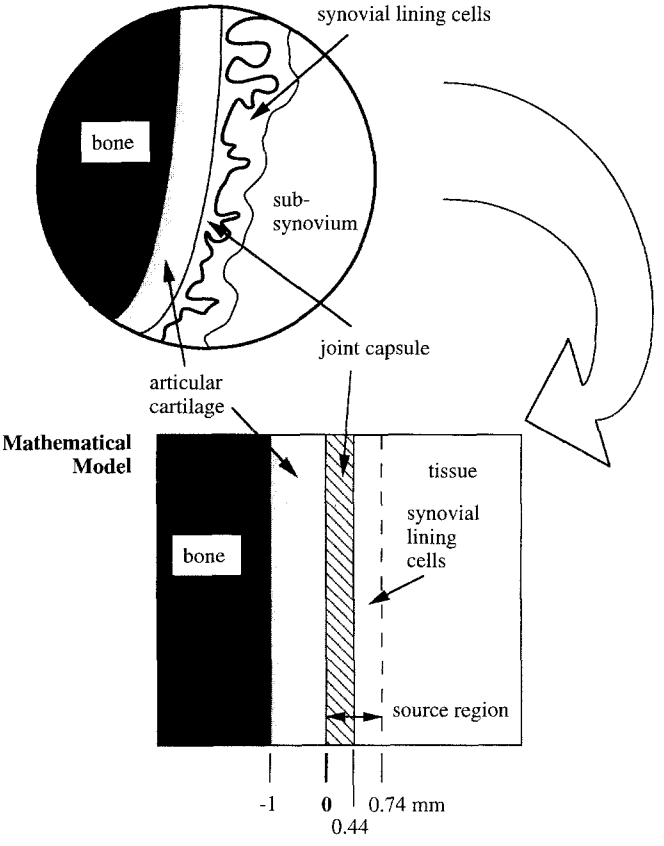

Fig. 1. Mathematical model of the rheumatoid synovial joint used in the Monte Carlo calculations. It is shown with an inset (*above*) illustrating the juxtaposition of relevant synovial joint tissues and the highly variable nature of convoluted synovium, which was considered to be too joint-specific to model explicitly. The model incorporates regions of bone, articular cartilage, joint capsule, and tissue (synovium). Injected radioactivity is assumed to be uniformly distributed throughout both the joint capsule and the synovial lining cells, situated along the synovial surface

soft tissue, which represents synovium. The synovium is subdivided into a surface layer of lining cells and underlying subsynovium.

The model's radiation source region includes both the joint capsule and synovial lining cells. Injected radioactivity was assumed to be uniformly distributed throughout this region. The joint capsule was modeled as a 0.44-mm-thick slab of water located between the articular cartilage and synovium. The lining cells were modeled as a 0.30-mm-thick slab of tissue along the synovial surface.

Computer simulations

Using the EGS4 Monte Carlo computer code [13], beta-particle emission from within the radiation source region and subsequent transport of the particles through the joint model was simulated, one radionuclide at a time. Simulation begins by choosing a starting position, direction, and energy for the emission of a single beta-particle from the decaying radionuclide. The starting position is a point randomly selected from the 0.74-mm-thick radiation source region (0.30 mm joint capsule plus 0.44 mm lining cells). The starting direction is chosen at random over 4π space. The initial kinetic energy of the emitted beta-particle is determined by randomly sampling the radionuclide's decay spectrum. Decay spectra of possible beta-particle emission energies are well documented for each of the radionuclides investigated [14].

The emitted beta-particle then is transported through the joint model by the EGS4 computer code. At each point in the particle's life where a choice of interaction type, scattering direction, distance to the next interaction, etc. has to be made, a random number is generated by the code and used to determine the event's outcome from known probability distributions which describe the behavior of real particles. Simulated interactions include all the major events, such as the production of secondary knock-on electrons and bremsstrahlung photons. "Continuous" energy loss and multiple scattering through weak interactions with atomic electrons also are taken into account. Simulation ends when the emitted beta-particle and all its secondaries no longer have enough energy to excite the absorbing media. At this point, a new beta-particle is "emitted" from within the radiation source region and the process is repeated.

During simulation, the code keeps track of the amount of energy deposited by the transported particles in each of the model's four absorbing media: bone, articular cartilage, the fluid-filled joint capsule, and tissue (representing synovium and subsynovium). To increase the spatial resolution of the results, these four absorbing media were subdivided into a total of 50 smaller bins. Energy deposited by the transported particles was tallied separately for each of the 50 bins.

Deposited energy was converted to an absorbed dose factor for each bin according to the following relation:

$$F_i = \Delta E_i \frac{\kappa}{\Delta T_i \rho_i N}, \tag{1}$$

where F_i is the absorbed dose factor for the i^{th} bin (cGy-cm^2/MBq-s), ΔE_i is the energy deposited in the bin (MeV), κ is a unit conversion constant, ΔT_i is the thickness of the bin (cm), ρ is the density of the absorbing medium in the bin (g/cm^3), and N is the number of nuclear disintegrations, integrated over time (MBq-s). Nuclear disintegrations which do not result in the emission of beta-particles were taken into account (through the incorporation of a multiplication factor describing the fraction of nuclear disintegrations which results in the emission of a beta particle).

The outermost bins were each 0.25 mm thick, while the innermost bins were generally 0.20 mm thick. Two exceptions were the two joint capsule bins, which were each 0.22 mm thick, and the lining cells bin, which was 0.30 mm thick.

Dose estimates

Radiation doses throughout treated joints can be estimated as a function of time using the absorbed dose factors described above. For any location in the joint model and at any time t after injection, the radiation absorbed dose from injected radioactivity is calculated as the product of the cumulated activity $\tilde{A}(t)$ in the source region and the bin's absorbed dose factor F_i divided by an estimate of the joint's total synovial surface area S_{syn}, so that:

$$D_i(t) = \frac{\tilde{A}(t) F_i}{S_{syn}}. \tag{2}$$

The cumulated activity after time t is given by:

$$\tilde{A}(t) = \frac{A_0}{\lambda_P}(1 - e^{-\lambda_P t}), \tag{3}$$

where A_0 is the activity initially deposited in the source region and λ_P is the injected radionuclide's physical decay constant.

For a very long time relative to the half-life, Eq. 3 reduces to $\tilde{A}(t)=A_0/\lambda_P$, and the total dose D_i becomes:

$$D_i = \frac{A_0 F_i}{\lambda_P S_{syn}}. \tag{4}$$

A very long time relative to the half-life, for most purposes, can be taken to mean any time t greater than six half-lives, which for the short-lived emitters commonly used in radiation synovectomy is on the order of 1–20 days.

Although leakage of radioactivity from the joint was not included in the computer simulations directly, accommodations for leakage can be made in the dose estimates. For instance, to accommodate a reduction in dose due to leakage of activity from the joint, the physical decay constant in Eq. 3 can be replaced with an effective decay constant λ_E. Physically, it represents the length of time required for one-half the radioactivity present to be removed through the combined effects of leakage and radioactive decay. The resulting equation for estimating absorbed dose distributions in treated joints as a function of time is given by:

$$D_i(t) = \frac{A_0 F_i}{\lambda_E S_{syn}}(1 - e^{-\lambda_E t}). \tag{5}$$

The activity required to deliver a prescribed synovial dose to the i^{th} bin $D_i(t)$ (accommodating leakage) can be determined by solving Eq. 5 for A_0.

Dose rate estimates

Dose rates throughout treated joints also can be estimated using the absorbed dose factors described above. The initial dose rate $\dot{D}_i(0)$ from injected radioactivity to any location i in the joint model, for instance, is calculated as:

$$\dot{D}_i(0) = \frac{A_0 F_i}{S_{syn}}. \tag{6}$$

And dose rates at later times t are given by:

$$\dot{D}_i(t) = \frac{A_0 F_i}{S_{syn}}(1 - e^{-\lambda_E t}), \tag{7}$$

where λ_E is the effective decay constant.

Simulation parameters

Use of the EGS4 code requires the user to input values for various parameters. All simulations described here were run with the list of parameters values shown in Table 1. For discussions on the influence of each of these parameters on the calculated results, readers are referred to the EGS4 literature. In particular, the EGS4 code manual (distributed by the Radiation Shielding Information Center, Oak Ridge National Laboratory) [13] and a text on the Monte Carlo transport of electrons and photons, edited by Jenkins, Nelson, and Rindi [15], provide extensive coverage of the topic.

Uncertainty

Typical estimates of uncertainty in the calculated values of F_i were 1%–2% in the bins nearest (within 2 mm of) the source region and 5%–10% in the bins farther (greater than 2 mm) from the source region. The uncertainty was estimated by dividing the total number of starting particles into four equal groups. Energy deposition for each group was scored separately. At the end of simulation, the results were used to calculate an average absorbed dose factor F_i and associated standard deviation for each bin.

Phantom experiments

Ultrathin radiachromic film dosimeters were used to measure depth-dose data in joint phantoms built to resemble the mathematical joint model as closely as is possible. Tissue substitutes used in the phantom included aluminum as a substitute for bone (commonly used in experimental electron dosimetry) [16] and solid water as a substitute for articular cartilage and soft tissue (synovium).

Solid water is an epoxy resin-based material specially formulated to have electron and photon absorption and scattering characteristics very similar to those of water [17]. Use of water substitutes as soft tissue substitutes for the purposes of dosimetry is not expected to introduce uncertainties in the absorbed dose estimates greater than 1%. Using a homogeneous, cubic, solid water phantom (30 cm×30 cm×30 cm) and a ^{60}Co source, Constantinou et al. measured depth-dose data within ±1% of those derived for a standard water phantom [18]. Solid water also has been shown to be superior to other commonly used water substitutes, e.g., Lucite and polystyrene [17].

Table 1. Parameter values used in the EGS4 simulations

Parameter	Value used
Maximum energy loss per step (ESTEPE)	0.02 (2%)
Lower energy for electron data (AE)	1 keV
Lower energy for photon data (AP)	1 keV
Upper energy for electron data (UE)	10 MeV
Upper energy for photon data (UP)	10 MeV
Electron cutoff energy (ECUT)	10 keV
Photon cutoff energy (PCUT)	10 keV
Number of histories	100000
IRAYL	1
IAPRIM	1

Joint phantom

The assembled joint phantom is illustrated in Fig. 2. On one side of the radioactive source (described below), several slabs of aluminum (each 1 mm thick) were stacked together and served as a substitute for bone. A single slab of solid water (1 mm thick) positioned between the aluminum slabs and the radioactive source served as an articular cartilage substitute, to mimic the layer of articular cartilage that caps the ends of the bones in all synovial joints.

On the other side of the radioactive source, several slabs of solid water (each 1 mm thick) were stacked together and served as a substitute for soft tissue (synovium). In the phantom, distances are defined in relation to the leftmost solid water/radioactive source interface, as indicated in Fig. 2.

Radioactive source preparation

Planar sources of ^{165}Dy and ^{166}Ho were prepared to closely resemble the model's radioactive source region. In the model, radioactivity was assumed to be uniformly distributed throughout both the 0.44-mm joint capsule and the 0.30-mm lining cells layer. The density thickness of the source in the model was equal to 74 mg/cm^2. The sources were prepared as follows.

^{165}Dy. Planar sources of ^{165}Dy with initial radioactivity on the order of 9000 MBq were prepared by dipping ten thin squares of cellulose filter paper, each 7.5 mg/cm^2 thick and 6 cm×6 cm in area, once each in a solution containing 1.75 mg Dy_2O_3 (stable, natural dysprosium) dissolved in 5.0 ml nitric acid (3% HNO_3). The soaked papers were dried in air by hanging them vertically but rotating them each a few times in the vertical plane while drying in order to achieve greater uniformity in the distribution of dysprosium on the papers. Ten filter papers were used so that the density thickness of the experimental source would approximate that of the mathematical model; the density of cellulose was taken to equal 0.5 g/cm^3. The 5.0 ml volume of solution was chosen so that

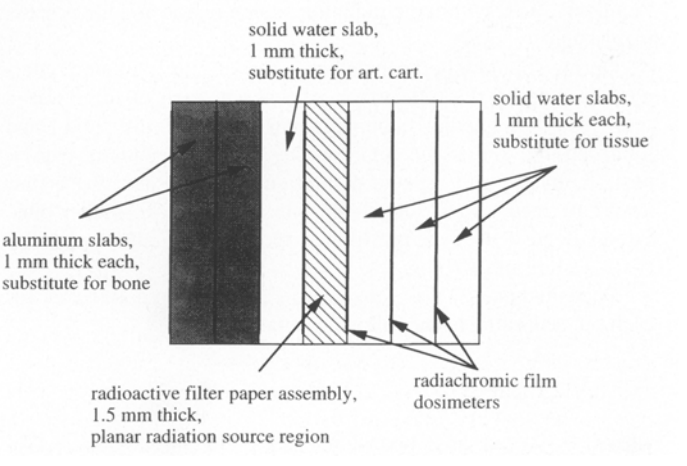

Fig. 2. Joint phantom used to experimentally measure radiation absorbed dose distributions of reactor-produced ^{165}Dy and ^{166}Ho. Tissue substitutes in the phantom included aluminum as a substitute for bone and solid water as a substitute for articular cartilage and tissue (synovium). Depth-dose data were measured using radiachromic film dosimeters. Distances in the phantom are defined in relation to the leftmost solid water/radioactive source interface

all the liquid was absorbed by the ten filter papers and the last filter paper was uniformly wet.

When the papers had dried, they were stacked and stitched together at the four corners using a needle and thread. The dried filter paper assembly then was irradiated at the MIT Nuclear Reactor Laboratory (Cambridge, Mass.) for 54 min at full power (thermal neutron flux $\approx 7.5\times10^{12}$ neutrons/cm^2–s). Activation of stable ^{164}Dy on the papers resulted in the production of roughly 8.6×10^3 MBq ^{165}Dy. After allowing 80 min decay time for radiation protection purposes, the filter paper assembly was inserted into the joint phantom. At the time of insertion, the activity of ^{165}Dy in an assembly was estimated to equal 5.0×10^3 MBq. This activity was allowed at least ten half-lives to decay before being removed from the phantom. ^{165}Dy has a 2.3-h half-life.

^{166}Ho. A planar source of ^{166}Ho with initial radioactivity of 250 MBq was prepared following the procedures described above for ^{165}Dy, with the following exceptions. One mg Ho_2O_3 (stable, natural holmium) was dissolved in 5.0 ml nitric acid (3% HNO_3), and this solution was used to soak the filter papers. In addition, the irradiation time was 6 h, instead of 54 min.

Activation of stable ^{165}Ho on the papers resulted in the production of 250 MBq ^{166}Ho. After allowing 2 h of decay time for radiation protection purposes, the 240 MBq ^{166}Ho remaining on the papers was inserted into the joint phantom. The activity was allowed at least ten half-lives to decay. ^{166}Ho has a 27-h half-life.

Dosimeters

GafChromic DM1260 radiachromic film dosimeters (purchased from Far West Technology, Inc., Goleta, Calif.) were used to measure absorbed dose as a function of position in the phantom. The film is a thin, laminated plastic material having radiation absorption properties similar to those of soft tissue. It consists of a very thin ($\approx$7 μm thick) radiachromic sensor coating (a proprietary substance) on a polyester film base ($\approx$100 μm thick). When exposed to ultraviolet or ionizing radiation with energy greater than 4 eV, the coating undergoes a radiation-induced color change by photoionization [19, 20]. The change, from colorless to deep blue, occurs as a function of absorbed dose and requires no processing. Dosimetric characteristics of the film include: a linear response to ionizing radiation over a wide range of absorbed doses; dose-rate independence; energy independence of response down to a few keV; an equivalent response to electrons and photons; low atomic number composition (primarily H, C, N, O); and the fact that the radiation-induced image is quite stable [21].

A major advantage of the radiachromic film dosimetry system is the straightforward manner in which the radiation response is analyzed. A reader designed specifically for standard radiachromic film dosimetry is a simple photometer. Light, filtered to the film's peak absorption wavelength, is transmitted through the dosimeter, where it is received by a silicon photodiode and converted into an electrical signal. The signal is fed into a high input impedance operational amplifier, and the output is displayed on a meter as optical density. Optical density (OD) is related to transmission according to the following relation:

$$\mathrm{OD} = \log\frac{T_0}{T}, \tag{8}$$

where T_0 is 100% transmission and T is transmission after coloration. A calibration curve depicting the change in optical density (ΔOD) as a function of absorbed dose D is used to quantify the dose imparted to the dosimeters (see below).

Portions of a 12.7-cm-wide roll of GafChromic film were cut into 6 cm×6 cm squares for insertion into the joint phantom. The size of the film squares was large enough so that four 1 cm×1 cm samples cut from the center were separated from any edges by at least 1.5 times the range of the most energetic beta-particle emitted, a distance which is sufficiently large to prevent boundary, or edge, effects in the measurements.

The cut film squares were sandwiched between the slabs of aluminum and solid water, at each of the positions shown in Fig. 2. Upon the insertion of a radioactive source, the films were used to measure the absorbed dose deposited at each of these positions, or depths, in the phantom.

Calibration. Since the film's change in optical density for a given absorbed dose is strongly dependent on the thickness of the sensor coating, which varies from batch to batch, each batch of films must be calibrated individually. The calibration curve for the film used in these experiments was generated by first irradiating samples of the film with known radiation doses, then measuring the change in optical density and plotting the results. The irradiations were conducted under controlled conditions using gamma radiation from a calibrated ^{60}Co source at the National Institute of Standards and Technology (Bethesda, Md.). Samples of the film were sealed inside polymer-aluminum laminate packets, held between two 5.0-mm polystyrene blocks, and irradiated to doses of 100, 200, 400, 700, or 1000 Gy. Estimates of uncertainty in the delivered doses are less than 3%.

The change in optical density then was measured for each of the irradiated dosimeters and used to calculate a calibration curve for the film. The calibration curve relating the absorbed dose D in Gy to a measured change in optical density ΔOD is as follows:

$$D=10.2(\Delta\mathrm{OD})^3+27.3(\Delta\mathrm{OD})^2+290\Delta\mathrm{OD}. \tag{9}$$

All absorbed dose measurements in this work were obtained with a readout wavelength of 600 nm.

Analysis

After each of the radioactive sources was inserted and allowed ten half-lives to decay, the joint phantoms were disassembled and the radiachromic film dosimeters were retrieved for analysis. Four 1 cm×1 cm samples were cut from the center of each dosimeter. For each sample, the change in optical density ΔOD was measured and converted to an absorbed dose D using the above calibration curve (see Eq. 9).

In each of the experiments, absorbed dose D was measured at six depths, or positions: −1.0 mm, 0.0 mm, 0.74 mm, 1.74 mm, 2.74 mm, and 3.74 mm. Four absorbed dose measurements were obtained at each position, and the average dose was converted to an absorbed dose factor according to the following relation:

$$F_i = \frac{D_i \lambda S_{source}}{A}, \tag{10}$$

where F_i is the absorbed dose factor (cGy-cm^2/MBq-s) at position i, D_i is the average absorbed dose (Gy) measured at position i, λ is the radionuclide's decay constant (s^{-1}), S_{source} is the surface area of the radioactive filter paper assembly (36 cm^2), and A is the amount of radioactivity (MBq) on the filter papers upon insertion into the phantom.

The inserted radioactivity A was estimated according to the following relation:

$$A=n\sigma\phi(1-e^{-\lambda t_1})(1-e^{-\lambda t_2}), \tag{11}$$

where n is the number of target nuclei on the filter paper assembly, σ is the thermal neutron activation cross-section (cm^2), ϕ is the thermal neutron flux (cm^{-2}-s^{-1}), λ is the radionuclide's physical decay constant (s^{-1}), t_1 is the length of irradiation (s), and t_2 is the length of time between irradiation and insertion (s). In each experiment, the entire mass of Dy_2O_3 or Ho_2O_3 in the 5.0 ml solution was assumed to be absorbed by the ten filter papers and uniformly distributed on them.

Cadaver experiments

Cadavers

Four knees, cut from mid-thigh to mid-calf, were obtained from freshly frozen cadavers at the Harvard Medical School (Boston, Mass.). None of the knees had evidence of structural joint changes associated with rheumatoid arthritis. Knees 3 and 4 were obtained from the same cadaver. In each of the specimens, the suprapatellar pouch was found to be intact and thus did not appear to present a path for leakage of injected radioactivity away from the joint.

Dosimeters

GafChromic DM1260 radiachromic film dosimeters were cut into 1 cm×4 cm strips and wrapped in clear plastic tape to prevent them from getting wet. The size of the strips was large enough to allow three absorbed dose measurements per strip.

Implantation

In each of the four knees, a 15 cm midline incision was made from a distal point just medial to the tibial tubercle to a proximal point along the thigh midline and superior to the patella. The medial subcutaneous tissue then was raised to reveal the medial retinaculum and the vastus medialis obliquus. The exposed quadriceps tendon was cleared of overlying fat, and a standard medial parapatellar arthrotomy was performed, i.e., the joint capsule was cut open. Then the patellofemoral ligament was cut; the patella, everted; and the knee, flexed approximately 90°.

Next the radiachromic film dosimeters were stitched into five strategic locations through-out the joint capsule using silk sutures. The locations were: in the posterolateral corner adjacent to the popliteus hiatus, in the posteromedial corner just anterior to the posterior capsule, adjacent to the anterior cruciate ligament, in the lateral gutter of the suprapatellar pouch, and on the deep surface of the quadriceps tendon (as listed in Table 2). At the latter three sites, the films were secured with additional silk sutures. The knees then were closed and sewn tight at three separate layers.

It is important to note that all the dosimeters were positioned on the synovial surface and none were placed at depth in bone, articular cartilage, or tissue (due to problems associated with the accurate positioning of dosimeters to within a few millimeters of the radioactive source region). As a consequence, the cadaver experiments did not provide the data necessary to complete a full comparison with the Monte Carlo results. Instead, aims of the cadaver experiments included comparing the synovial surface dose with that predicted using Monte Carlo and examining the spatial distribution of injected radioactivity in the treated joint.

Table 2. Joint locations at which radiachromic film dosimeters were positioned to measure absorbed dose in the knees of cadavers

Joint location	Description
A	Posterolateral corner
B	Posteromedial corner
C	Adjacent to anterior cruciate ligament
D	Lateral gutter
E	Deep surface of quadriceps tendon

Injection

A therapeutic dose of ^{165}Dy ferric hydroxide macroaggregate was prepared for injection following standard clinical procedures [22]. The amount of prepared activity was measured using a dose calibrator (Capintec, Inc., Ramsey, N.J.).

Using a 3-cc syringe attached to a three-way stopcock, each of the knees was injected with radioactive ^{165}Dy through a superolateral arthrocentesis portal, and the needle track was flushed with 1.5 ml saline. The knees were manipulated through two complete ranges of motion in an effort to distribute the injected radioactivity throughout the joint as uniformly as possible. The knees were left alone for 24 h to allow time for the radioactive dysprosium to decay.

Gamma camera imaging

At 16 h after injection, planar images of the injected knees were obtained using a gamma camera (Picker Dyna) set to image the 90 keV ^{165}Dy gamma-ray (emitted in 3.6% of the decays) with a 128×128 pixel matrix. The camera's collimator was rotated 180°, covered with an absorbent vinyl pad, and positioned so that the knees could be placed directly on top of it for static images. The imaging time was 10 min.

Analysis

At 24 h after injection, the knees were reopened, and the dosimeters were retrieved for analysis. The method used to analyze the dosimeters in the cadaver experiments was identical to that used in the phantom experiments.

In each of the four experiments, three absorbed dose measurements were obtained at each joint location. The average dose at each location then was converted to an average absorbed dose factor according to the following relation:

$$F_i = \frac{D_i \lambda S_{syn}}{A}, \qquad (12)$$

where F_i is the average absorbed dose factor (cGy-cm^2/MBq-s) at location i, D_i is the average absorbed dose (Gy) measured at location i, λ is the decay constant for ^{165}Dy ($8.37\times10^{-5}s^{-1}$), S_{syn} is an estimate of the total synovial surface area in the joint (≈250 cm^2), and A is the amount of injected radioactivity (MBq). In this case, A was experimentally measured using a dose calibrator.

Results

Monte Carlo simulations

Absorbed dose factors

Results of the Monte Carlo calculations are presented in Fig. 3 as absorbed dose factors (cGy-cm^2/MBq-s) versus

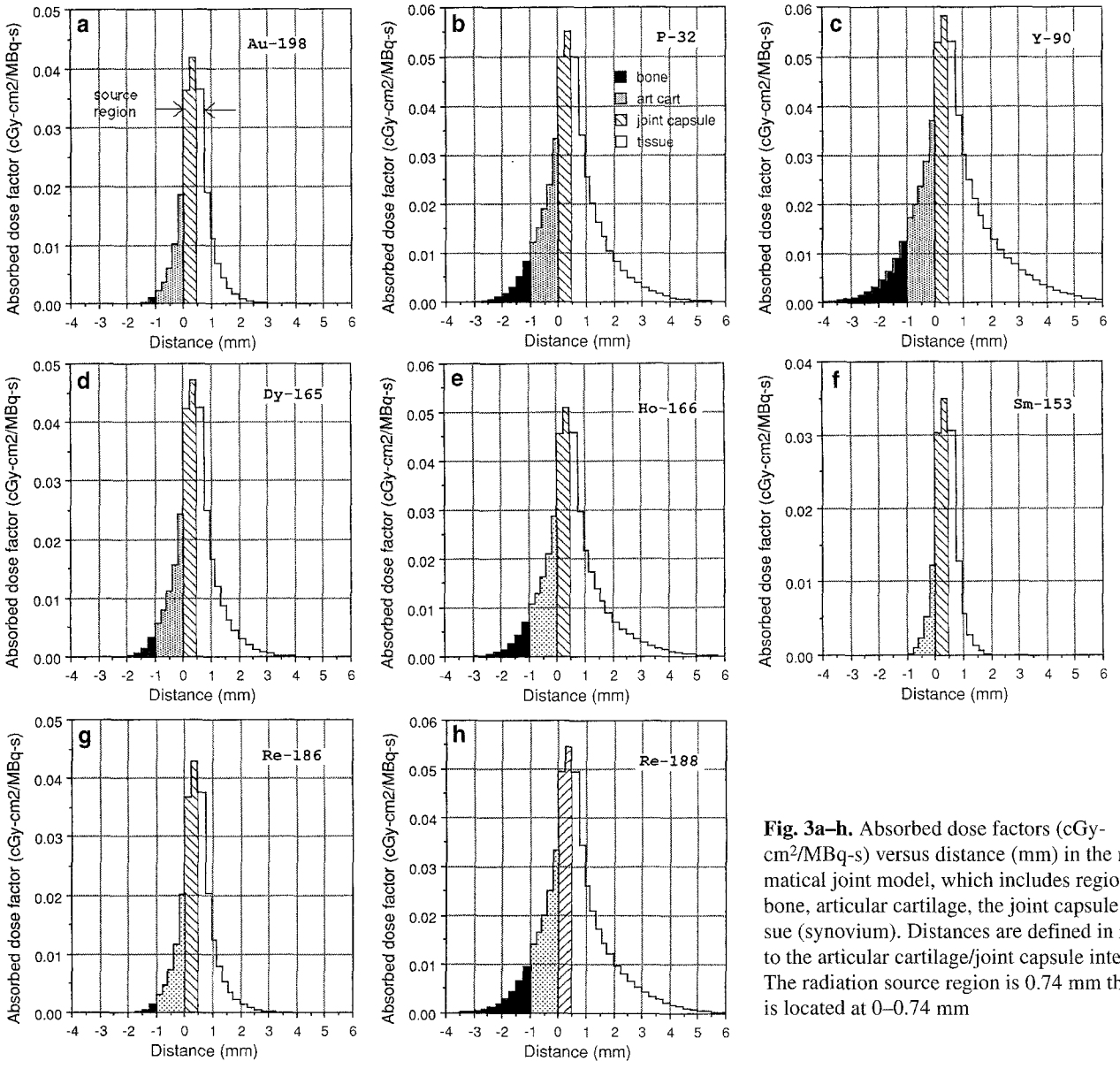

Fig. 3a–h. Absorbed dose factors (cGy-cm^2/MBq-s) versus distance (mm) in the mathematical joint model, which includes regions of bone, articular cartilage, the joint capsule, and tissue (synovium). Distances are defined in relation to the articular cartilage/joint capsule interface. The radiation source region is 0.74 mm thick and is located at 0–0.74 mm

depth in bone, articular cartilage, the joint capsule, and synovium. Beta dose distributions in treated joints can be extrapolated from the absorbed dose factors as described above. For example, consider the injection of 370 MBq (10 mCi) ^{198}Au into the knee, one of the earliest treatments reported to provide a beneficial effect in clinical trials [23]. If uniform distribution along 250 cm^2 of synovium is assumed [24], one can use Fig. 3 and Eq. 6 to calculate that the initial dose rate to the region of lining cells along the synovial surface is 0.55 mGy/s (200 rad/h); to the bone surface it is 0.03 mGy/s (9 rad/h). Integrating over time, the total dose to the lining cells is 1800 mGy (from Eq. 4), and to the bone surface it is 100 mGy.

The calculation assumes that all the ^{198}Au remains in the joint until decay. In practice, the potential for leakage from the joint via the lymphatic system always must be considered. Leakage, however, can be highly variable from joint to joint and from patient to patient. Dose estimates derived from the factors presented here therefore should be corrected for leakage on an individual basis (using Eq. 7).

Topp and Cross reported that for 18 knees the extra-articular leakage of ^{198}Au at 24 h after injection varied from as low as 1% of the injected activity to as high as 34% [25]. These data indicate that the biological half-life for removal of injected ^{198}Au from the joint varied from 1700 h down to 40 h (assuming first-order kinetics).

Continuing the sample calculation, for T_B equal to 1700 h the dose estimates remain unchanged. For T_B equal to 40 h, however, the corrected dose estimates for the lining cells and bone surface are 700 mGy and 40 mGy, respectively, which represent significant reductions in dose due to leakage of injected radioactivity away from the joint.

As another example, consider the injection of 74 MBq (2 mCi) ^{153}Sm into a smaller joint, e.g., the wrist. From Fig. 3, the ^{153}Sm absorbed dose factor for the lining cells is 0.031 cGy-cm^2/MBq-s. If uniform distribution along 50 cm^2 of synovial surface is assumed, the initial dose rate to the lining cells is 0.5 mGy/s (170 rad/h), from Eq. 6. Assuming no leakage, the total lining cells dose delivered over time is 1100 mGy, from Eq. 4.

Phantom experiments

The phantom experiments were conducted twice using ^{165}Dy sources and once using an ^{166}Ho source. The results are as follows.

^{165}Dy. Results of the two ^{165}Dy phantom experiments are shown in Table 3 as absorbed dose factors F_i (cGy-cm^2/MBq-s) at depth in the phantom. In each of the experiments, variations in measured doses D_i at each of the five positions were seen to be small, typically less than 5%. The small variations were attributed to the high precision of the radiachromic film dosimeters and the ease with which planar ^{165}Dy sources of uniform activity were made. Errors associated with the factors F_i shown in Table 3 are seen to be larger than 5%, however. The 15% errors shown in Table 3 are due primarily to uncertainties in accurately knowing the amount of radioactivity A inserted into the phantom in each of the two experiments. In Fig. 4 results of the two experiments are combined and compared with the Monte Carlo calculations for ^{165}Dy of absorbed dose factors versus depth in the mathematical joint model. Agreement between the EGS4 predictions and measured data is seen to be good.

^{166}Ho. Results of the ^{166}Ho phantom experiment are shown in Table 4. As in the ^{165}Dy experiments, variations in the measured doses D_i at each of the six positions were seen to be small, on the order of 5%. Due to uncertainties in accurately knowing the amount of ^{166}Ho radioactivity A inserted into the phantom, however, errors associated with the factors shown in Table 4 were estimated to be 15%. In Fig. 5, results of the phantom experiments are compared with the Monte Carlo calculations for ^{166}Ho. The agreement again is seen to be good.

Table 3. Results of the depth-dose measurements for ^{165}Dy obtained using the joint phantom. The results are expressed as absorbed dose factors (cGy-cm^2/MBq-s) at depth in the phantom

Phantom depth	Factor trial 1	Factor trial 2
−1.0 mm, bone surface	$5.1\times10^{-3}\pm15\%$	$4.4\times10^{-3}\pm15\%$
0.0 mm, art. cart. surface	$3.9\times10^{-2}\pm15\%$	$2.8\times10^{-2}\pm15\%$
0.74 mm, synovium at 0.3 mm	$4.1\times10^{-2}\pm15\%$	$2.8\times10^{-2}\pm15\%$
1.74 mm, synovium at 1.3 mm	$4.8\times10^{-3}\pm15\%$	$4.4\times10^{-3}\pm15\%$
2.74 mm, synovium at 2.3 mm	$8.4\times10^{-4}\pm15\%$	$8.2\times10^{-4}\pm15\%$

Table 4. Results of the depth-dose measurements for ^{166}Ho obtained using the joint phantom. The results are expressed as absorbed dose factors (cGy-cm^2/MBq-s) at depth in the phantom

Phantom depth	Factor
−1.0 mm, bone surface	$7.1\times10^{-3}\pm15\%$
0.0 mm, art. cart. surface	$3.3\times10^{-2}\pm15\%$
0.74 mm, synovium at 0.3 mm	$3.9\times10^{-2}\pm15\%$
1.74 mm, synovium at 1.3 mm	$8.3\times10^{-3}\pm15\%$
2.74 mm, synovium at 2.3 mm	$3.2\times10^{-3}\pm15\%$
3.74 mm, synovium at 3.3 mm	$1.1\times10^{-3}\pm15\%$

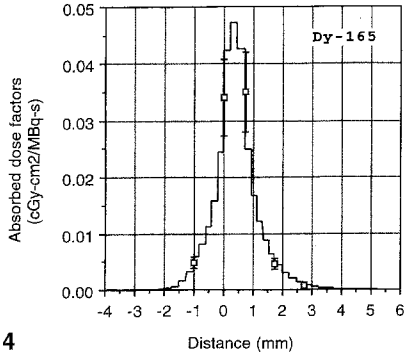

4

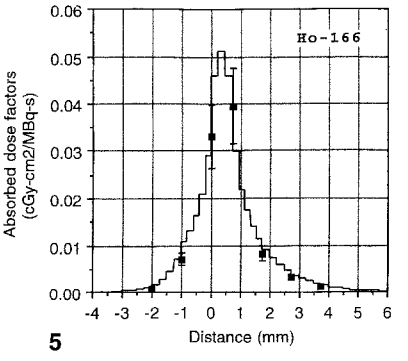

5

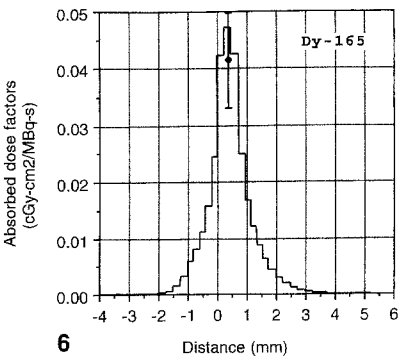

6

Fig. 4. Comparison of the absorbed dose factors derived from measurements obtained using ^{165}Dy sources in the joint phantom with those obtained using Monte Carlo radiation transport simulation in a mathematical model of the joint. The measured factors are shown as *data points* and include *error bars*; the factors calculated using Monte Carlo are shown as a *solid line*

Fig. 5. Comparison of the absorbed dose factors derived from measurements obtained using a ^{166}Ho source in the joint phantom with those obtained using Monte Carlo radiation transport simulation in a mathematical model of the joint. The measured factors are shown as *data points* and include *error bars*; the factors calculated using Monte Carlo are shown as a *solid line*

Fig. 6. Comparison of the absorbed dose factors derived from measurements made in the knees of cadavers with those obtained using Monte Carlo radiation transport simulation in a mathematical model of the joint. The measured factors are shown as *data points* and include *error bars*; the factors calculated using Monte Carlo are shown as a *solid line*

Table 5. Results of the absorbed dose measurements made at several strategic locations in the knees of cadavers. Each of the knees was injected with a therapeutic dose of ^{165}Dy. Results are listed as absorbed dose factors (cGy-cm^2/MBq-s) at each of the locations (see Table 2)

Location	Factor knee 1	Factor knee 2	Factor knee 3	Factor knee 4
A	$2.3\times10^{-2}\pm5\%$	$5.4\times10^{-3}\pm20\%$	$3.0\times10^{-2}\pm28\%$	$4.1\times10^{-2}\pm9\%$
B	$2.5\times10^{-2}\pm5\%$	0	$2.9\times10^{-2}\pm10\%$	$1.9\times10^{-2}\pm17\%$
C	$2.0\times10^{-2}\pm6\%$	$3.3\times10^{-3}\pm33\%$	$2.0\times10^{-2}\pm5\%$	$3.6\times10^{-2}\pm53\%$
D	$7.5\times10^{-2}\pm5\%$	$3.1\times10^{-2}\pm7\%$	$6.9\times10^{-2}\pm15\%$	$6.0\times10^{-2}\pm80\%$
E	$1.3\times10^{-2}\pm11\%$	$1.0\times10^{-1}\pm5\%$	$5.1\times10^{-2}\pm13\%$	$5.0\times10^{-2}\pm86\%$

Cadaver experiments

Results of the four cadaver experiments are shown in Table 5 as average absorbed dose factors (cGy-cm^2/MBq-s) at each of the five joint locations listed in Table 2. (Again, it is important to note that all the radiachromic film dosimeters were stitched to locations on the synovial surface, and that none were positioned at depth in bone, articular cartilage, or tissue. As a consequence, depth-dose data were not obtained in the cadaver experiments.)

Errors associated with the factors listed in Table 5 are seen to range from 5% to 86%. In this case, the uncertainty was due primarily to nonuniform distribution of injected radioactivity in the knees. Varying degrees of uniformity in the spatial distribution of injected radioactivity resulted in the wide range of uncertainties shown in Table 5.

In Fig. 6 results of the first and third cadaver experiments were compared with the Monte Carlo calculations for ^{165}Dy. Since each of the absorbed dose measurements was made at a point located on the synovial surface, all the results obtained in the cadaver experiments appear at the same position in the ^{165}Dy profile, i.e., on the synovial surface. Results of the second and fourth experiments were not included in the comparison due to the poor distribution of injected radioactivity in the knees. Gamma camera scans of the knees at 16 h after injection confirmed the unequal distribution.

Discussion

Beta-particle dosimetry in radiation synovectomy is a difficult problem for a variety of reasons. These include the physical difficulties associated with the beta-dosimetry of low-energy electrons in heterogeneous media and the biological and anatomical difficulties associated with: the nonuniform distribution of synovial lining cells in rheumatoid joints and the nonuniform distribution of radioactivity within them; leakage of radioactivity from the joint, which may be variable; uncertainties in knowing the surface area of the synovial membrane over which the administered activity is distributed; etc. [24]. The approach taken here was first to idealize the biological and anatomical factors, since they are so highly variable and difficult to determine on a patient by patient basis, and then to carry out Monte Carlo calculations coupled with experiments in joint phantoms and the knees of cadavers to address the physical difficulties and complete an accurate evaluation of beta-particle dosimetry in the idealized system.

Therapeutic range

The dose factors presented in Fig. 3 are intended to provide guidance for those interested in radionuclide selection, dose prescription, and resulting absorbed dose distributions in radiation synovectomy. Dependent on the thickness of synovium to be treated and the proximity of other, nontarget tissues, radionuclide selection is based, at least in part, on an evaluation of the absorbed dose penetration of potential radionuclides. In particular, one wants to ensure that the deepest limit of the target volume lies within a radionuclide's *therapeutic range* and that other, healthy structures located nearby (such as bone and articular cartilage) are not subjected to an unnecessary radiation hazard. The therapeutic range is defined as the depth at which the absorbed dose is equal to 10% of the maximum dose, deposited at the synovial surface.

Table 6 lists therapeutic and maximum ranges of the eight radionuclides investigated. In each case, the therapeutic range is seen to be much shorter than the maximum beta-particle penetration range. In addition, the eight therapeutic ranges are seen to demonstrate considerably less variation between radionuclides than the eight maximum ranges.

Since it is the therapeutic range which determines the synovial thickness that can be treated and not the maximum range, treatment volume variations between radionuclides are not large. In fact, six of the eight radionuclides investigated were seen to have a therapeutic range of roughly 1–2 mm, and none of them was seen to have a therapeutic range greater than 3 mm. Noting that suc-

Table 6. Therapeutic and maximum ranges of the eight radionuclides investigated

Radionuclide	Therapeutic range (mm)	Maximum range (mm)
^{32}P	2.2	7.9
^{90}Y	2.8	10.8
^{153}Sm	0.7	3.1
^{165}Dy	1.3	5.6
^{166}Ho	2.1	8.7
^{186}Re	1.0	4.5
^{188}Re	2.1	10.1
^{198}Au	0.9	3.9

cessful clinical results have been reported for several of these radionuclides, including both low- and high-energy emitters [2], it seems reasonable to conclude that the target volume in radiation synovectomy lies within a few millimeters of the synovial surface, and that a full-thickness synovectomy is not required to produce favorable results in patients. As a consequence, the commonly held hypothesis that only isotopes which emit high-energy beta particles can be used to treat large joints [26, 27] may need to be reconsidered.

It is interesting to note that during the 1970s, as ^{90}Y replaced ^{198}Au as the radionuclide of choice or rheumatoid knees, the 10 mm maximum penetration range of ^{90}Y often was named as a motivation for the switch [26, 27]. The 10 mm range refers to the radionuclide's maximum beta-particle penetration range, however, and not to its absorbed dose penetration range, which is closer to 3 mm. While it is true that clinical success rates did improve with the switch to ^{90}Y, this result now appears to have been influenced more strongly by an improved ability to control the particle size (and, hence, leakage) than by an increased penetration range.

Leakage

The problem of leakage of injected radioactivity away from joint generally is considered to be the primary disadvantage of existing radiation synovectomy procedures. Leakage rates in the past have been both high and highly variable, with up to 20%–50% of the injected radioactivity commonly reported to escape [28–31]. As shown above in the sample calculation for ^{198}Au, the corresponding effects on resulting absorbed dose distributions in leaky joints can be substantial. Assuming first-order kinetics, the sample calculation reveals that for ^{198}Au, given a leakage rate in which 34% of the injected radioactivity escapes during the first 24 h after injection, the corresponding reduction in absorbed dose to the synovial surface is roughly 60%, i.e., the synovial surface receives only 40% of the dose it would have received had the activity remained in the joint.

Given that leakage can have such large effects on resulting absorbed dose distributions, theoretical approaches to dosimetry which accommodate leakage are of interest. The approach taken here is to assume first-order kinetics and to incorporate a radiopharmaceutical's biological half-life into the dose calculations. The biological half-life is defined as the length of time required for one-half the activity present to be removed from the joint through biological pathways, as opposed to radioactive decay. In the clinic, it is envisioned that estimates of a particular radiopharmaceutical's biological half-life can be obtained using simple gamma camera scans to monitor leakage of radionuclides which emit accomanying gamma-rays or using more complex measurement conditions to count the bremsstrahlung photons of radionuclides which emit only beta-particles [27, 32].

Absorbed dose to nontarget tissues

The incidental irradiation of nontarget tissues, such as bone and articular cartilage, is unavoidable in radiation synovectomy as it is currently practiced. Absorbed dose imparted to the cartilagenous surfaces is especially large, as is indicated in the profiles shown in Fig. 3. It is worth noting, however, that these surfaces generally are not destroyed by the therapy, unless the amount of injected radioactivity is exceptionally large, e.g., 370 MBq (10 mCi) ^{90}Y. Damage to the articular surfaces has been reported for this particular amount of radioactive ^{90}Y injected into rheumatoid knees. Using the factors shown in Fig. 3, the corresponding dose to both the synovial and articular cartilages is roughly 2500 mGy. Injections of one-half this amount of ^{90}Y have been shown to be sufficient to provide patients with symptomatic relief of RA [33, 34].

While not as large as that to cartilage, absorbed dose to bone also is of interest in radiation synovectomy since the International Committee on Radiation Protection has identified the bone surface (10 μm) and the active, blood-forming red marrow as two principal radiosensitive targets to be protected in procedures involving bone irradiation [35]. For the radionuclides investigated here, dose to the bone surface is seen to vary from 25% of the lining cells dose for ^{90}Y, down to 4% for ^{186}Re and essentially 0% for ^{153}Sm. Dose to the blood-forming marrow is not considered to be as important, since it is located much further from the radioactive source region, on the order of centimeters, not millimeters. The authors know of no previous attempt to estimate nontarget tissue doses in radiation synovectomy.

Comment on the use of EGS4

EGS4 is one of a few well-known and highly sophisticated Monte Carlo codes which is capable of simulating electron transport through heterogeneous media. Although it originally was developed to study high-energy electromagnetic cascade showers, such as those produced at particle accelerators, the EGS code package recently has been modified to extend its useful range to include lower energies.

Because of its high-energy origin, where forward scattering dominates, the latest version of the code has been described as suffering from a number of inherent "weaknesses" associated with its condensed history transport of low-energy electrons: multiple scattering according to the theory of Móliere, bremsstrahlung differential in energy only, and a simple treatment of low-energy electrons and photons. As a consequence, further improvements to the code have been made, mainly through the inclusion of user-defined restrictions in the electron step-sizes (variable name ESTEPE) to yield a more accurate system. Other additions include electron transport down to 10s of keV, Rayleigh scattering (i.e.,

coherent photon scattering), and bremsstrahlung differential in angle, as well as energy.

In the present work, the aim of the experimental dosimetry in phantoms and cadavers was to verify the accuracy of the resulting EGS4 electron transport code package, i.e., the default version of EGS4 with the inclusion of the improvements named above, as used here in the dosimetry of low-energy electrons in heterogeneous media. These comparisons are discusssed, in turn, below.

Comparison of Monte Carlo with measured data in phantoms

Referring to Figs. 4 and 5, median values of the absorbed dose factors obtained in both the ^{165}Dy and ^{166}Ho phantom experiments are seen to be in good agreement with the corresponding EGS4 estimates of beta-dose penetration in the mathematical joint model. The agreement seems to indicate that use of EGS4 to evaluate the dosimetry of low-energy electrons (<2 MeV) in heterogeneous media is an acceptable application of the code. Unfortunately, these measured data alone cannot be used to make a more definitive statement on the topic since the uncertainty associated with each of the experiments is plus or minus 15%.

In the phantom experiments, the principal source of error in the experimental data arose from uncertainty in accurately knowing A, the amount of radioactivity on the filter paper assembly upon insertion into the phantom. Since we did not possess the capability to measure A, it was estimated instead, assuming that all the Dy_2O_3 or Ho_2O_3 was absorbed by the filter papers and uniformly distributed on them. This source of uncertainty could be reduced if one had the ability to measure A just before inserting the radioactive papers into the phantom.

Comparison of Monte Carlo with measured data in cadavers

In Fig. 6, the median value of the synovial surface dose obtained from measured data in the knees of cadavers is seen to be in good agreement with that predicted using EGS4. Again, the agreement indicates that the beta-dose distributions predicted using EGS4 indeed may be accurate. However, the large error bar associated with the result prohibits one from making a more definitive statement.

The error in this case results from difficulties associated with the nonuniform distribution of injected activity in the knees. Poor distribution is recognized as being a formidable problem in radiation synovectomy. In the clinic, commonly used efforts to improve distribution include subjecting the joint to a few range-of-motion exercises before immobilization and carefully controlling the particulate size. The data shown in Table 5 indicate the magnitude of the problem in a worst case scenario, i.e., with no phagocytic absorption of injected radioactivity by the synovial membrane. In knee 2, for example, joint location B (postero-medial corner) was seen to receive no beta-dose, while location E (deep surface of quadriceps tendon, and the location closest to the point of injection) was seen to receive a relatively large dose.

The distribution was seen to be much better in knees 1 and 3, which had average absorbed dose factors of $3.1\times10^{-2}\pm15\%$ cGy-cm^2/MBq-s and $4.0\times10^{-2}\pm36\%$ cGy-cm^2/MBq-s, respectively. In patients, the distribution is expected to be better still, due to active absorption and retention of injected radioactivity by the synovial lining cells.

Comparisons with other published data

There have been only a few attempts to derive theoretical estimates of beta-dose distributions in radiation synovectomy [5, 24, 25]. Of these, the most detailed calculation was by Husak et al., who assumed that radionuclides injected into the rheumatoid joint are absorbed by the synovial surface and are uniformly distributed over it so that a thin plane source of activity is formed [24]. They then applied the beta dose point kernel method to determine the dependence of absorbed dose in tissue on distance (up to 0.6 mm) from thin plane sources of ^{198}Au and ^{90}Y.

Agreement between the results of Husak et al. and those presented here is good. For ^{198}Au, for instance, Husak et al. calculated that 37 MBq (1 mCi) uniformly distributed on a synovial surface area of 250 cm^2 delivers an absorbed dose at 0.15 mm of approximately 180 mGy (1800 rad), integrated over all time. The corresponding value of absorbed dose estimated using the dose factors for ^{198}Au shown in Fig. 3 is 182 mGy. For 37 MBq (1 mCi) ^{90}Y on a surface area of 250 cm^2, they reported an absorbed dose to tissue at 0.15 mm of approximately 250 mGy. Using the dose factors in Fig. 3, an absorbed dose of 262 mGy is determined in the present work. Differences in the estimates of absorbed dose for the two approaches are 1% for ^{198}Au and 5% for ^{90}Y. Additional comparisons with Husak et al. of absorbed dose at depth are not made since their curves do not continue beyond 0.6 mm.

While the agreement with Husak et al. indicates that their approach was a good one, the absorbed dose factors presented here represent an improvement for a number of reasons. These include the facts that the curves shown in Fig. 3 present results for eight radionuclides of interest (not only two), extend beyond 0.6 mm, include regions of bone and articular cartilage, and provide users with the option of incorporating the effects of leakage.

Conclusion

Beta-particle dosimetry of various radionuclides used in the treatment of rheumatoid arthritis was estimated using

Monte Carlo radiation transport simulation coupled with experiments using reactor-produced radionuclides and radiachromic film dosimeters. Results were presented as absorbed dose factors (cGy-cm^2/MBq-s) at depth in bone, articular cartilage, the joint capsule, and synovium, and can be used to extrapolate beta dose distributions in treated joints.

Definite data on the absorbed dose required at depth in synovium for successful therapy have not been established. In fact, the rationale for choosing a particular administered dose of a given radionuclide in a given joint remains obscure; and most published studies have relied on historically derived, "empirical" dosimetry. However, for a given areal concentration of injected radioactivity uniformly distributed throughout the joint capsule and along a surface layer of lining cells, absorbed doses to tissue (synovium), articular cartilage, and bone are easily estimated with the results shown in Fig. 3. Ultimately, it is expected that the results of this work will provide a detailed, accurate, and useful account of radiation absorbed dose distributions in radiation synovectomy.

References

1. Fellinger K, Schmid J. Die lokale Behandlung der rheumatischen Erkrankungen. *Wien Z Inn Med* 1952; 33: 351.
2. Deutsch E, Brodack JW, Deutsch KF. Radiation synovectomy revisited. *Eur J Nucl Med* 1993; 20: 1113–1127.
3. Harbert JC. *Nuclear medicine therapy.* New York: Thieme Medical, 1987.
4. Webb FWS, Lowe J, Bluestone R. Uptake of colloidal radioactive yttrium by synovial membrane. *Ann Rheum Dis* 1969; 28: 300–302.
5. Ingrand J. Characteristics of radio-isotopes for intra-articular therapy. *Ann Rheum Dis* 1973; 32 Suppl: 3–9.
6. Bowen BM, Darracott J, Garnett ES, Tomlinson RH. Yttrium-90 citrate colloid for radioisotope synovectomy. *Am J Hosp Pharm* 1975; 32: 1027–1030.
7. Shortkroff S, Jones AG, Sledge CB. Radiation synovectomy. In: *Advances in metals in medicine.* JAI Press; 1993: 155–186.
8. Noble J, Jones AG, Davis MA, Sledge CB, Kramer RI, Livni E. Leakage of radioactive particle systems from a synovial joint studied with a gamma camera: its application to radiation synovectomy. *J Bone Joint Surg [Am]* 1983; 65: 381–389.
9. Sledge CB, Noble J, Hnatowich DJ, Kramer R, Shortkroff S. Experimental radiation synovectomy by 165-Dy ferric hydroxide macroaggregate. *Arthritis Rheum* 1977; 20: 1334–1342.
10. Shortkroff S, Mahmood A, Sledge CB, Jones AG, Brodack JW, Chinen LK, Deutsch E, Deutsch KF. Studies on Ho-166-labeled hydroxyapatite: a new agent for radiation synovectomy. *J Nucl Med* 1992; 33: 937.
11. Brodack JW, Chinen LK, Deutsch E, Deutsch KF. Studies on the radiolabeling of hydroxyapatite particles for use as radiation synovectomy agents. *J Nucl Med* 1992; 33: 980.
12. Johnson LS, Yanch JC. Absorbed dose profiles for radionuclides of frequent use in radiation synovectomy. *Arthritis Rheum* 1991; 34: 1521–1530.
13. Nelson WR, Hirayama H, Rogers DWO. *The EGS4 code system.* Stanford Linear Accelerator Center, 1985.
14. Hogan OH, Zigman PE, Mackin JL. *Beta spectra II. Spectra of individual negatron emitters.* United States Radiological Defense Laboratory, 1964.
15. Jenkins TM, Nelson WR, Rindi A, eds. *Monte Carlo transport of electrons and photons.* New York: Plenum Press, 1987.
16. *ICRU-44: tissue substitutes in radiation dosimetry and measurement.* International Commission on Radiation Units and Measurements, 1989.
17. Constantinou C. *Tissue substitutes for particulate radiations and their use in radiation dosimetry and radiotherapy.* PhD thesis, University of London, 1978.
18. Constantinou C, Attix FH, Paliwal BR. A solid water phantom material for radiotherapy x-ray and γ-ray beam calibrations. *Med Phys* 1982; 9: 436–441.
19. Chalkley L, Phototrophy. *Chem Rev* 1929; 6: 217.
20. McLaughlin WL, Chalkley L. Measurement of radiation dose distributions with photochromic materials. *Radiology* 1965; 84:124.
21. Humphreys KC, Kantz AD. Radiachromic: a radiation-monitoring system. *Radiat Phys Chem* 1977; 9: 737–747.
22. Hnatowich DJ, Kramer RI, Sledge CB, Noble J, Shortkroff S. Dysprosium-165 ferric hydroxide macroaggregates for radiation synovectomy. *J Nucl Med* 1978; 19: 303–308.
23. Ansell BM, Crook A, Mallard JR, Bywaters EGL. Evaluation of intra-articular colloidal gold Au-198 in the treatment of persistent knee effusions. *Ann Rheum Dis* 1963; 22: 435–439.
24. Husak V, Wiederman M, Kral M. Absorbed dose due to beta-rays from radioactive colloids in radiation synovectomy. *Phys Med Biol* 1973; 18: 848–854.
25. Topp JR, Cross EG. The treatment of persistent knee effusions with intra-articular radioactive gold. *CMA Journal* 1970; 102: 709–714.
26. Prichard HL, Bridgman JF, Bleehan NM. An investigation of radioactive yttrium (^{90}Y) for the treatment of chronic knee effusions. *Br J Rheum* 1970; 43: 466–470.
27. Gumpel JM, Williams ED, Glass HI. Use of yttrium 90 in persistent synovitis of the knee. I. Retention in the knee and spread in the body after injection. *Ann Rheum Dis* 1973; 32: 223–227.
28. Gumpel JM, Beer TC, Crawley JC, Farran HE. Yttrium 90 in persistent synovitis of the knee: a single center comparison of four radiocolloids. *Br J Radiol* 1975; 48: 377–381.
29. Oka M, Rekonen A, Routsi A, Seppala O. Intra-articular injection of Y-90 resin colloid in the treatment of rheumatoid knee effusions. *Acta Rheumatol Scand* 1971; 17: 148–160.
30. Deckart H, Tamaschke J, Ett S, Tautz M, Knapp G. Radiosynovectomy of the knee joint with gold-198 colloid, yttrium-90 ferric hydrate colloid and rhenium-186 sulphide colloid. *Radiobiol Radiother (Berlin)* 1979; 3: 363–370.
31. Virkkunen M, Krusius FE, Keiskanen T. Experiences of intra-articular administration of radioactive gold. *Acta Rheumatol Scand* 1967; 13: 81–91.
32. Kyle V, Hazelman BL, Wraight EP. Yttrium-90 therapy and Tc- 99m pertechnetate knee uptake measurements in the management of rheumatoid arthritis. *Ann Rheum Dis* 1983; 42: 132–137.
33. Spooren PFMJ, Rasker JJ, Arens RPJH. Synovectomy of the knee with ^{90}Y. *Eur J Nucl Med* 1985; 10: 441–445.
34. Will R, Laing B, Edelman J, Lovegrove F, Surveyor I. Comparison of two yttrium-90 regimens in inflammatory and osteoarthropathies. *Ann Rheum Dis* 1979; 38: 45–47.
35. *ICRP-26: recommendations of the ICRP.* International Commission on Radiation Protection, 1977.